Monitoring of IR Clear-sky Radiances over Oceans for SST (MICROS): Near-Real Time Web-Based Tool for Monitoring CRTM – AVHRR Biases

Xingming Liang[1,2*] and Alexander Ignatov[1]

[1] NOAA/NESDIS, Center for Satellite Application and Research (STAR), Camp Springs, MD 20746
[2] CSU, Cooperative Institute for Research in the Atmospheres (CIRA), Fort Collins, CO 80523

Abstract

Monitoring of IR Clear-sky Radiances over Oceans for SST (MICROS, www.star.nesdis.noaa.gov/sod/sst/micros/) is a web-based tool developed at NESDIS to monitor the "model minus observation" biases in clear-sky brightness temperatures (BT) over oceans. MICROS employs the newly developed Advanced Clear-Sky Processor for Oceans (ACSPO), which became operational in May 2008. ACSPO generates AVHRR clear-sky BTs, sea surface temperature (SST), and aerosol products from NOAA-16, -17, -18, and MetOp-A. The central part of ACSPO is the fast Community Radiative Transfer Model (CRTM), which is used in conjunction with Reynolds SST and Global Forecast System upper-air data to simulate clear-sky BTs in the AVHRR thermal bands centered at 3.7, 11, and 12 μm. This paper documents the MICROS system and discusses effects of three ACSPO versions on the stability of the global BT and SST biases. ACSPO upgrades did not significantly affect the global mean biases, but their standard deviations have significantly improved. Double-differencing technique is employed to check clear-sky BTs over ocean for cross-platform consistency. Robust statistics have been recently added to MICROS, in addition to conventional statistics. All analyses show that BTs are generally stable and cross-platform consistent to within several hundredths of a degree Kelvin except for NOAA-16. The largest bias, ~-0.11 K, is observed in NOAA-18 Ch4 relative to NOAA-17 Ch4. For accurate cloud masking and physical SST retrievals, biases in AVHRR BTs should be fully understood and minimized. Work is also underway to include monitoring of clear-sky BTs from NOAA-19/AVHRR, MSG/SEVIRI, NPOESS/VIIRS and GOES-R/ABI in MICROS.

1. Introduction

Advanced Clear-Sky Processor for Oceans (ACSPO) was developed in NESDIS and became operational in May 2008 with AVHRR Global Area Coverage (GAC) data from NOAA-18 and MetOp-A. Data from NOAA-16 and -17 are also processed to better understand and improve the ACSPO performance. The major ACSPO products are clear-sky brightness temperatures (BTs) over ocean in all AVHRR bands, sea surface temperatures (SST), and aerosols. Also, clear-sky BTs in AVHRR Ch3B, Ch4, and Ch5 are simulated using the fast Community Radiative Transfer Model (CRTM; Kleespies et al., 2004; Han et al., 2006) and reported in ACSPO product granules, side-by-side with AVHRR measured clear-sky BTs. Implementation of CRTM in ACSPO in conjunction with Reynolds SST and National Centers for Environmental Prediction (NCEP) Global Forecast System (GFS) upper air fields, and its validation against nighttime AVHRR radiances, has been documented in Liang et al. (2009). CRTM BTs are used in ACSPO to explore physical SST retrievals, improve cloud detection, and evaluate quality of sensor

* *Corresponding author address: Xingming Liang, NOAA/NESDIS/STAR, WWB Rm. 603, 5200 Auth Rd, Camp Springs, MD 20746; e-mail: Xingming.Liang@noaa.gov*

radiances and CRTM performance. Near-real time (NRT) monitoring of the model (CRTM) minus observation (AVHRR), or M-O, BT biases is critically important for these applications.

Monitoring of IR Clear-sky Radiances over Oceans for SST (MICROS, www.star.nesdis.noaa.gov/sod/sst/micros/) was established in July 2008 to evaluate the BT (model minus observation, $\Delta T_B = T_{CRTM} - T_{AVHRR}$) and SST (satellite minus Reynolds, $\Delta T_S = T_S - T_R$) biases in the ACSPO product. Since then, MICROS has been employed to validate and improve the CRTM (Liu et al, 2009). This paper additionally demonstrates the utility of MICROS to test out new versions of ACSPO and to monitor satellite radiances over clear-sky global ocean for stability and cross-platform consistency, in NRT.

Currently, MICROS performs three functions: it runs ACSPO for NOAA-16, -17, -18, and MetOp-A (note that MICROS can also work with ACSPO granules generated offline); performs statistical analyses of the ACSPO products; and displays their summary results on the web. This processing is done fully autonomously in the Center for Satellite Applications and Research (STAR), independently of the operational ACSPO processing performed by the Office of Satellite Data Processing and Distribution (OSDPD), also a part of NESDIS. MICROS version 1.0 was implemented in July 2008, initially based on ACSPO v1.00. In September 2008, ACSPO in MICROS was upgraded to v1.02 and in November 2008, to v1.10. In December 2008, MICROS was updated to version 2.0, in which the web interface was restructured and more analyses added. Currently, MICROS runs in NRT, once a day, after one full day of AVHRR Level 1B data have been accumulated. MICROS results are displayed on the web page lagging AVHRR L1b data acquisition by ~24 hours.

This paper describes results of monitoring the BT and SST biases in different versions of ACSPO using MICROS. Section 2 describes MICROS, section 3 describes the three ACSPO versions covered by MICROS from July to December 2008, and section 4 evaluates stability of the global BT and SST biases. Analyses of cross-platform consistency using double-differencing technique are discussed in Section 5, concluding with a summary of the paper and outline of future work in section 6.

2. MICROS

Currently, MICROS runs daily. First, ACSPO processing starts at ~2:00 am EST after all corresponding L1B data for a full previous day have been accumulated. Processing runs on a local STAR Linux box with four 2.33 GHz CPUs and 4 GB memory. GAC L1b data from NOAA-16, -17, -18, and MetOp-A are processed and 1-hr ACSPO granules generated. These granules contain AVHRR and CRTM BTs; retrieved and Reynolds SSTs; and cloud mask in each GAC pixel, among other variables. ACSPO processing takes ~3 minutes per platform and per orbit, and there are from 14 to 15 L1b GAC orbits per platform, per day. Thus, the total ACSPO processing time for four platforms is close to 3 clock hours (3 min × 14 orbits × 4 platforms).

Once ACSPO granules have been generated, they are statistically processed and results are displayed on the web. The global statistics include histograms of ΔT_B and ΔT_S, from which global daily mean and SD are calculated. Time series of these parameters are also plotted in

order to monitor the BT and SST biases for long-term stability. Double-differencing technique (explained later in section 5) is employed in MICROS to evaluate the biases for cross-platform consistency. Global maps of the biases and corresponding geophysical and environmental parameters are also calculated and displayed. Dependencies on the main factors affecting the BT and SST biases, such as the column water vapor content, view zenith angle, wind speed, Reynolds SST, air-sea temperature difference, and latitude, are also produced. Robust statistics including median and robust standard deviation (RSD) have been also added in MICROS v2.0 to minimize the effect of possible outliers in the data on the evaluation of CRTM and AVHRR radiances (cf., Merchant et al., 2008). The conventional statistics are also kept as they are representative of the actual performance of the current ACSPO product. Statistical analyses are performed in the full retrieval domain and all results are displayed in the MICROS page, with no exemption or additional quality control other than the ACSPO cloud mask. In particular, data in the full swath ±68° are analyzed. The Interactive Data Language (IDL) code takes half an hour of clock time to perform statistical analyses for one full day of data from four satellites.

All analyses are performed separately for day and night. At this time, nighttime analyses are more accurate and appropriate for the validation of CRTM and satellite radiances. For daytime data, treatment of solar reflection in CRTM v1.1 (employed in ACSPO v1.10) remains suboptimal. In particular, the relative azimuth angle dependence is still not included in the calculations (Liu, 2008). As a result, the current daytime analyses in MICROS show anomalous behavior. Work is underway with the CRTM team to improve and validate the CRTM daytime calculations. Although the daytime data are also reported in MICROS for completeness and to provide a benchmark for evaluating future CRTM improvements, only nighttime results are analyzed in this paper.

3. ACSPO Versions Tested in MICROS

Since MICROS was introduced in July 2008, it proved instrumental to quickly evaluate and test all new ACSPO developments. This study documents results of testing three ACSPO versions: v1.00 (employed in MICROS from 1 July to 3 September, 2008), v1.02 (4 September to 11 November, 2008), and v1.10 (13 November 2008 to present). Note that only v1.00 and v1.10 have been officially implemented in the NESDIS OSDPD operations, whereas v1.02 remained internal to the ACSPO development team at STAR. Nevertheless, it provided a critical update to ACSPO and, therefore, was separately tested in MICROS and documented here. This section provides a brief overview of ACSPO versions, which is essential for interpreting the results observed in the MICROS web page. Also, these ACSPO upgrades provide a natural way to estimate the stability and improvements in the ACSPO BT and SST biases.

3.1 Major features of ACSPO v1.00, v1.02 and v1.10

Major features of ACSPO v1.00 have been described in Liang et al. (2009). To summarize, it used an alfa-version of CRTM (termed "r577") in conjunction with NCEP/GFS upper air data and Reynolds weekly 1º SST (OISST.v2, Reynolds et al., 2002). Also, it employed an initial version of ACSPO cloud mask documented in Petrenko et al. (2008).

In ACSPO v1.02 implemented in MICROS on 4 September 2008, a number of critical changes have been made. First, weekly 1° Reynolds OISST.v2 was replaced with a daily 0.25° product (Reynolds et al, 2007). Two daily Reynolds SST products are available. One is based on blending NAVOCEANO AVHRR SST product (May et al., 1998) with *in situ* SST; hereafter, it is termed "Reynolds daily (AVHRR)." The other product additionally uses retrievals from the Advanced Microwave Scanning Radiometer flown onboard Aqua satellite since 2002. It is termed "Reynolds daily (AVHRR+AMSR)". The AMSR has an all-weather advantage as clouds are essentially transparent to microwave radiation. However, the coarser AMSR footprint may affect SST accuracy in the coastal areas (Reynolds et al, 2007). Users of ACSPO 1.02 and later versions have a choice of using three SST inputs: weekly, daily (AVHRR), or daily (AVHRR+AMSR) Reynolds SSTs.

Another critical update in ACSPO v1.02 was replacing CRTM r577 with the official CRTM version 1.1. Also, the default CRTM surface model based on Wu-Smith (1997) wind-speed-dependent emissivity is now used instead of Fresnel's model employed in Liang et al. (2009). Finally, the more accurate transmittance coefficient data for the wide band are used (referred to as "Planck-Weighted," or PW coefficients, e.g., Chou et al., 1993; Turner, 2000; Chen, 2007) instead of the "ordinary" (ORD) coefficients released in CRTM r577. Note that the PW coefficients are only employed for NOAA-17, -18, and MetOp-A. Our analyses of NOAA-16 Ch3B (not shown) reveal an unrealistic "out of family" negative M-O bias when PW coefficients are used. This fact may be attributable to the out of band effect in its spectral response (Liu et al., 2009). Work is underway with CRTM team to resolve this anomaly in NOAA-16 Ch3B. In the meantime, the ORD coefficients for NOAA-16 (all bands) are kept in ACSPO v1.02 and v1.10. Additionally, although the improvement resulting from using PW instead of ORD coefficients is expected to be largest in AVHRR Ch3B compared to Ch4 and Ch5 (Chen, 2007), our analyses suggest that the effect of using PW coefficients is more complex. More comprehensive analyses of PW vs. ORD coefficients are currently underway and their results will be reported elsewhere.

ACSPO v1.10 further improved cloud detection by using flexible band and sensor-specific cloud filters, which are further stratified by day and night (Petrenko et al., 2009). Also, the threshold at which the day/night flag switches over was changed from the solar zenith angle of 85º (in ACSPO v1.00 and 1.02) to 90º (in v1.10). The new v1.10 has further improved characterization of the global BT biases for the use in the cloud mask, relative to v1.02.

In the following subsections, we focus on three sensitivity analyses to evaluate the effects on the global BT biases when ACSPO versions have changed from v1.00 to v1.02 to v1.10. Additionally, the improvements resulting from using an updated cloud mask in ACSPO v1.10 has been also evaluated in detail by Petrenko et al. (2009) for a few case studies.

3.2 Using Daily Instead of Weekly SST in ACSPO v1.00

There are two critical changes from ACSPO v1.00 to v1.02. This subsection documents evaluating the effect of using Reynolds daily SST instead of weekly SST on global BT biases. The effect of the CRTM version upgrade will be discussed in section 3.3 below.

Figures 1-3 (a-b) quantify the improvements resulting from using Reynolds daily SST (AVHRR) instead of weekly SST using NOAA16-18 and MetOp-A Ch3B data for 12 July 2008. Using daily Reynolds SST as input to CRTM significantly reduces the global SD compared to using weekly SST. However, the mean bias increases by ~+0.08 K. As discussed in Liang et al. (2009), increased bias may not necessarily be "bad" news here as it leaves a wider margin for future model improvements (including incorporation of aerosols in the CRTM, using skin SST instead of current bulk, and adjusting "daily mean" Reynolds SST for a diurnal cycle to represent nighttime conditions) as well as for an improved ACSPO cloud masking. Note that the effect of using daily Reynolds SST is largest in the higher latitudes of both hemispheres and over some coastal areas. Recall that the ACSPO cloud mask uses CRTM BTs (Petrenko et al., 2008, 2009), which in turn use Reynolds SST as input. The fact that the clear-sky ocean domain does not change significantly when weekly SST is replaced with daily product suggests that the ACSPO cloud detection algorithm is largely insensitive to the SST input to CRTM. The view zenith angle dependencies in Figure 3b form a tighter cluster compared with Figure 3a, but the amplitude of the angular dependencies remains largely unchanged. Additional analyses of daily AVHRR+AMSR SST as CRTM input were performed but they did not show any significant difference compared to the case of using daily (AVHRR) SST (results not shown here). AVHRR-based Reynolds daily SST was selected for the use in ACSPO as it is less dependent on the external microwave data (AMSR) and is thus more robust and uniform in time, offering a better potential for future climate reprocessing of AVHRR data using ACSPO.

3.3 CRTM Updates in ACSPO v1.02

Figures 1, 2, and 3 (c) show the same data set as in Figures 1, 2, and 3 (b) but processed with the new CRTM formulation used in ACSPO v1.02. For the sake of this sensitivity study, the daily Reynolds (AVHRR) SST was used in both panels (b) and (c), and only CRTM formulation has changed. The new CRTM formulation adopted in ACSPO v1.02 includes using CRTM v1.1, the built-in Wu-Smith emissivity model, and Planck-Weighted coefficients for NOAA-17, -18, and MetOp-A. (Recall that the CRTM formulation adopted in ACSPO v1.00 used CRTM r577, Fresnel's emissivity model, and ORD coefficients.) The new CRTM formulation slightly increases clear-sky coverage as manifested by the larger N values overlaid in Figure 1 (c). The SDs of the M-O BT biases slightly deteriorate for NOAA-18 and improve for NOAA-17 and MetOp-A, but they significantly improve for NOAA-16. Interestingly, the mean biases for NOAA-17, -18, and MetOp-A are now reduced by ~-0.08 K. Additional analyses (not shown) suggest that this change is mainly due to using PW instead of ORD coefficients. Note that the decrease of ~-0.08 K offsets the previous ~+0.08 K gain from using daily Reynolds SST, making the net balance of both changes in global mean BT bias close to zero (but leaving the global SD significantly improved). The fact that the global BT bias is less sensitive to view zenith angle in Figure 3c compared to Figure 3b indicates that using the wind-speed dependent Wu-Smith (1997) emissivity model is more accurate than Fresnel's model used in ACSPO v1.00. Recall, however, that in the current CRTM version, both emissivities are used in CRTM in conjunction with the downwelling radiance coming from a fixed direction of 53º. Using a more physical formulation is expected to further improve the BT biases, especially at the edges of scan (e.g., Watts et al., 1996). Work is underway with the CRTM team to fix this incorrect formulation (Liang et al., 2009).

Figure 1 (b) shows that in ACSPO v1.00, NOAA-16 Ch3B was biased low with respect to the other three platforms by ~-0.3 K (cf. Liang et al., 2009). This bias is not observed if the new CRTM formulation is used. By working with the CRTM team, it was found that the reason was the suboptimal treatment of atmospheric layers above the top GFS layer of 10 mbar in CRTM r577, which has led to a stronger than expected effect of the out-of-band contribution in NOAA-16 Ch3B spectral response function on CRTM forward calculations (Liu et al., 2009). This problem was fixed in CRTM v1.1.

3.4 Improvements in ACSPO v1.10

The same data set used in Figures 1 through 3 (a–c) was processed using ACSPO v1.10, and the results are shown in Figures 1 through 3 (d). Compared to v1.02, the number of clear-sky observations is significantly reduced. This change is in part due to the change in the day/night flag from 85° (in ACSPO v1.00/1.02) to 90° (in v1.10). This nighttime reduction is partially compensated by the increase in the daytime sample size. The compensation is not full though, due to the additional updates in the cloud mask (Petrenko et al., 2009). The global mean biases in ACSPO v1.10 for MetOp-A, NOAA-17 and -18, and their corresponding SDs, have consistently reduced compared to v1.02. Unlike other platforms, the global mean biases and SDs for NOAA-16 slightly increase in ACSPO v1.10. This anomaly in NOAA-16 will be further discussed in section 4.5 below. The amplitude of the view zenith angle dependencies is reduced in ACSPO v1.10.

Overall, analyses in this section show that all the performance metrics employed in MICROS consistently indicate gradual improvements in the consecutive ACSPO versions. The major advantage of these checks is that they are performed in NRT and allow to quickly measure product improvements.

4. Stability of Nighttime BT and SST Biases

In this section, the stability of nighttime BT and SST biases is evaluated. Conventional (mean and SD) and robust (median and RSD) statistics are employed to emphasize two different aspects. The robust statistics are more informative of the CRTM and sensor calibration performance, whereas the conventional statistics are more sensitive to outliers and thus are more representative of the actual product performance (e.g., Merchant et al., 2008, 2009). Proximity between the conventional and robust statistics is thus a sensitive indicator of the overall ACSPO product's well-being.

4.1 Global Mean Biases

Time series of the global mean BT and SST biases are shown in Fig. 4 (left panel). For all platforms except NOAA-16, the BT biases are ~+0.2 K in Ch3B, and ~+0.5 K in Ch4 and Ch5. The warm biases are likely due to a combined effect of aerosols (which are not accounted for in the current CRTM version); using bulk SST instead of skin; and using "daily-mean" Reynolds SST to represent the nighttime SST, which is cooler due to the effect of the diurnal cycle. Also, ambient and residual cloud affects BT biases. All these effects, if included or corrected for, would lower the BT biases and bring them closer to the expected "zero" state (Liang et al., 2009).

However, simultaneous reconciliation of all different AVHRR bands may be challenging, because most of these factors are expected to be either comparable in different AVHRR bands or larger in Ch3B.

ACSPO SST is biased cold during nighttime by several tenths of a degree Kelvin. Note that the blended Reynolds SST product is produced by bias-correcting satellite data to match, on average, the *in situ* SSTs. It is therefore expected that globally, Reynolds SST is centered on the *in situ* SST, so that the global mean "ACSPO minus Reynolds" bias should well represent the "ACSPO minus *in situ*" bias. In the initial ACSPO versions discussed here, the SST formulation was intentionally preserved from the heritage Main Unit Task (MUT) NESDIS SST system (Ignatov et al., 2004) for quick cross-evaluation of the two SST products. During nighttime, the following triple-window Multi-Channel SST (MCSST) equation is employed:

$$T_s = a_0 + a_1 T_{3b} + a_2 T_4 + a_3 T_5 + [a_4 (T_{3b} - T_5) + a_5](\sec\theta - 1) \quad (1)$$

The SST coefficients (a_0, a_1, a_2, a_3, a_4, and a_5) in ACSPO have been adopted from MUT without change (Dash et al., 2009). Note that during nighttime, MUT selects the warmest AVHRR pixel within a collocated High-Resolution Infra-Red Radiation Sounder (HIRS) footprint, which likely results in a warm bias in the MUT nighttime BTs. Using coefficients tuned against these "warm-biased" MUT BTs is expected to result in cold-biased ACSPO SSTs, which are derived from all clear-sky AVHRR pixels. Optimization of ACSPO regression SST is currently underway, and the improved SST formulations will be reported elsewhere.

There were no significant changes in the mean M-O bias in any band of any platform, when the ACSPO version was upgraded from v1.00 to v1.02 on 4 September 2008. This apparent lack of sensitivity is in fact due to a complex compensation between the two mechanisms, offsetting each other. Indeed, previous analyses discussed in section 3 show that using daily instead of weekly Reynolds SST increases the M-O bias in Ch3B by ~+0.08 K, while using the CRTM v1.1 offsets it by ~-0.08 K (cf. Figs. 1-3). Also, the BT and SST biases did not change noticeably when ACSPO v1.10 was introduced, a remarkable result considering a significant adjustment in the ACSPO cloud mask (Petrenko et al., 2009). The only exception is NOAA-16, for which the SST bias drops by ~-0.4 K and the M-O bias in Ch3B increases by ~+0.3K. This NOAA-16 anomaly is further discussed in section 4.5 below.

Global mean ΔT_B and ΔT_S biases experience long-term excursions with amplitude of ~±0.1 K. The BT oscillations are coherent in all AVHRR bands and for all platforms, and they occur in anti-phase with the SST oscillations. Their amplitude is largest in SST, followed by the most transparent Ch3B and then by Ch4 and Ch5. Note, for instance, a strong "hump" in ΔT_B ~-0.2 K in Ch3B and ΔT_B ~-0.1 K in Ch4 and Ch5 in early October 2008, and several smaller humps (about half as deep) in late July and mid-October 2008. There are always corresponding "bumps" found in the SST biases in Fig. 4g. These non-uniformities are likely caused by the instabilities in Reynolds SST used as input to CRTM. Small instabilities in the GFS fields are also possible but their effect on BTs in the window channels is expected to be much smaller. More analyses are needed to understand and reduce the effect of this "noise" in prior fields on the time series of BT and SST biases.

4.2 Time Series of Standard Deviations

Fig. 5 (left panel) shows global SDs of the BT and SST biases corresponding to Fig. 4. Unlike the global mean biases, the SDs of both ΔT_B and ΔT_S were significantly reduced when ACSPO was upgraded from v1.00 to v1.02. This is mainly due to using a more contemporaneous Reynolds 0.25° daily SST with higher spatial and temporal resolution instead of the 1° weekly SST, which is always available in ACSPO in a delayed mode (next day for the daily product and next week for the weekly product). The global SDs have reduced to 0.5 K in SST and Ch3B, 0.55 K in Ch4, and 0.65 K in Ch5 in ACSPO v1.02, and further improved in v1.10.

Note that before 4 September 2008, the global SDs showed a prominent weekly cycle, which was largest in the SST, followed by the most transparent Ch3B and then by Ch4 and Ch5. (Note that corresponding cycles were also observed in the mean ΔT_B and ΔT_S biases in Fig. 3, although not as clearly as in the global SDs.) This periodicity was an artifact of using weekly Reynolds SST in ACSPO v1.00, which was resolved when daily SST was employed in ACSPO v1.02.

4.3 Number of Nighttime Observations in ACSPO

Figure 6 shows time series of the number of clear-sky nighttime AVHRR GAC pixels over oceans within 24-hour time intervals from which statistics in Figs. 4 and 5 were generated. In ACSPO v1.00, from 2.5 to 3 million clear-sky ocean pixels have been used, and the update to v1.02 did not significantly change this number. However, in ACSPO v1.10, the number of clear-sky nighttime observations has reduced by about 20%. As discussed in section 4.2 above, this is in part due to the change of the day/night flag and is partially compensated by the increase in daytime sample size in v1.10. Note that drop-out points are due to the L1B data, which were unavailable in time for MICROS processing on some days.

4.4 Global Median Biases and RSDs

The global median and RSD of BT and SST biases are also shown in the right panels of Figs. 4 and 5. The difference between the global mean and median biases was largest before 4 September 2008 when ACSPO v1.00 was used, and it is reduced in ACSPO v1.02 and v1.10 (Fig. 4). The improved agreement between SD and RSD in the latter ACSPO versions is even more clear (Fig. 5). The closer agreement between the conventional and robust statistics indicates improved quality of the newer ACSPO products. The remaining differences between the conventional and robust statistics in ACSPO v1.10 suggest that the current ACSPO system still has room for improvement. In particular, including aerosol, using skin SST (instead of bulk), adjusting input SST to account for the effect of diurnal cycle, and further improvements to the cloud mask, CRTM, and sensor radiances are expected to better reconcile the conventional and robust statistics.

4.5 Anomalous Behavior of NOAA-16

NOAA-16 biases are unstable, in all bands. Recall that NOAA-16 currently flies close to the terminator and its AVHRR black body experiences significant impingement from the solar radiation (Cao et al., 2001; 2004b). This affects calibration in all AVHRR bands with the effect

expected to be largest in Ch3B. Recall also that the AVHRR sensor on NOAA-16 has experienced continuous problems since September 2003 and has not been used in NOAA operations after NOAA-18 was launched in May 2005. We have opted to include data from NOAA-16 in the MICROS analyses to better understand the performance of the ACSPO system in atypical situations. Work is underway to attribute the root causes of the observed NOAA-16 anomalies and correct them if possible. Results of these analyses will be reported elsewhere.

One change in NOAA-16 Ch3B bias in ACSPO v1.02, when the new CRTM v1.1 was implemented, has been already discussed in Section 3 and documented in details in Liu et al. (2009). Fig. 4a shows that after being in-family for about a month, Ch3B has developed a new low bias of ~-0.1 K in early October 2008 relative to the three other platforms. On the other hand, median statistics in Fig. 4b indicate that NOAA-16 is much closer to family. Analyses of the histogram of the BT biases (not shown) confirm that NOAA-16 biases have been highly non-Gaussian during this period of time.

When the new ACSPO v1.10 was implemented in MICROS on 12 November 2008, the global NOAA-16 BT biases in Ch3B jumped up by ~0.15 K. This increase is due to a combined effect of the new cloud mask and day/night flag change in ACSPO v1.10 (Petrenko et al., 2009). Work is underway to better understand and attribute the anomalous behavior of NOAA-16 in ACSPO.

5. Cross-Platform Consistency Using Double-Differencing Technique

Cross-platform consistency of BT biases independently verifies consistency of calibrations and spectral response functions between different sensors. Furthermore, continuous monitoring can help to evaluate whether this consistency is maintained in time. Although the M-O biases are non-zero and band-specific, they should closely agree between the two platforms, especially if the satellites overpass at the same local time. NOAA-17 and MetOp-A are currently flying very close orbits and cross the equator nearly simultaneously at ~21:50 local time, whereas NOAA-18 crosses the equator at ~1:40 a.m. and NOAA-16 at ~5:00 a.m. During this time range, the diurnal cycle in SST typically does not exceed ~0.1 K (e.g., Garand, 2003; Stuart-Menteth et al., 2005; Kennedy et al., 2007; Gentemann and Minnett, 2008) and therefore nighttime BT biases from all platforms are expected to be within several hundredths of a degree Kelvin, somewhat larger in Ch3b and smaller in Ch4 and Ch5, in proportion to the atmospheric attenuation in different bands.

Cross-platform consistency can be evaluated directly from Fig. 4. However, the excessive noise in the data prevents accurate quantitative analyses. In MICROS version 2, the double-differencing (DD) technique was adopted to rectify the cross-platform signal from noise. The satellite-to-satellite BT and SST DDs are respectively defined as follows:

$$SAT - REF = SAT[-(M - O)] - REF[-(M - O)] \quad (2)$$

$$SAT - REF = SAT[REG - REYNOLDS] - REF[REG - REYNOLDS] \quad (3)$$

Here, REF denotes a reference satellite, REG-REYNOLDS denotes SST mean bias (regression minus Reynolds SST), and SAT-REF denotes the cross-platform biases with respect to the reference. In MICROS, NOAA-17 was selected as a reference satellite because its

AVHRR sensor has been exemplarily stable. Also, NOAA-17 flies very close in time to MetOp-A, so that the corresponding DD signal should be minimally affected by the diurnal cycle. Note that the full global retrieval domains were used in calculating DDs, and the satellite footprints in the two datasets may not be completely co-located in space and time. The different clear-sky coverage for a pair of platforms may introduce day-to-day noise in the DD analyses although it is expected to largely cancel out in a global domain, depending on the accuracies of AVHRR data and CRTM input data, such as GFS and Reynolds SST. Work is under way to check the effect of the differences in the clear-sky domains in a pair of platforms on the DDs, and its results will be reported elsewhere.

The DD technique has been successfully used, for instance, to establish a calibration link between the Atmospheric Infrared Sounder (AIRS) and the Infrared Atmospheric Sounding Interferometer (IASI) sensors using GOES (Wang et al., 2009) or radiative transfer model simulation (Strow et al., 2008) as a transfer standard, and to establish inter-calibration links between the *Terra* and *Aqua* MODIS instruments using AVHRR/NOAA-17 as a reference (Wu et al., 2008). Similarly to the Strow et al. study (2008), the CRTM is used in MICROS as a transfer standard. The DD technique minimizes the effects on the BT artifacts that arise from such factors as errors in the reference SST or GFS upper air data, incomplete inputs to CRTM (such as missing aerosol), possible systemic biases in the CRTM forward model, and the updates to the ACSPO processing algorithm. Furthermore, the effects of all these factors may change in time. The DD largely cancels out these unknown, uncertain, or unstable factors and is thus expected to be more effective to cross-calibrate different sensors.

Figure 7 shows time series of the DDs for the mean and median BT and SST biases for NOAA-16, NOAA-18, and MetOp-A relative to NOAA-17. All data are smoothed by a three-day moving averaging filter to reduce noise resulting from the unstable global sample, which changes from day to day. Two flat lines represent the means of NOAA18 and MetOp-A DD biases to help emphasize cross-platform inconsistency. Note that in this paper, we only focus on the mean biases between the different platforms. In the future when longer time series are accumulated, linear trends may be considered. As discussed earlier, a large fraction of the "noise" in the BT and SST biases comes from the same source (such as errors in Reynolds SST or GFS data, CRTM or ACSPO versions, and missing aerosol). These factors are correlated between different platforms and cancel out when DD is calculated. MetOp-A is consistent with NOAA-17 to within several hundredths of a degree Kelvin, in all bands. The agreement between NOAA-18 and NOAA-17 is generally worse. Recall that NOAA-18 lags NOAA-17 by ~3 hours and therefore it is expected to be biased slightly low, due to the diurnal cooling. This diurnal signal should be largest in SST (<0.1 K) and progressively smaller in Ch3B, Ch4, and Ch5, respectively. Clearly, the different bands of NOAA-18 do not follow this expected pattern, suggesting that its calibration or spectral response function likely deviate from those assumed in the MICROS analyses and contribute to the DD signals. The largest difference is observed in Ch4, where NOAA-18 is significantly cooler than both NOAA-17 and MetOp-A. MetOp-A and NOAA-17 SSTs are expected to be consistent but show a difference of ~0.09 K, implying that the SST regression coefficients used in ACSPO (which, recall, were directly adopted from the NESDIS heritage MUT system) may not be fully accurate and should be improved. A similar bias was also found in the MUT SST analysis (Dash et al., 2009). The DDs also further emphasize and better quantify the instability in all bands of NOAA-16.

The SDs of the DDs, σ, are also listed in Fig. 7. They can be used to estimate the uncertainties of the respective mean DDs. The standard error of the mean of an ensemble of N measurements is $\sigma/\sqrt{N}$. The time series in Fig. 7 include half a year of data, ~180 days, but since three-day averaging was employed here, the number of independent observations should be effectively reduced by a factor of three, so that N~60. For instance, standard error of the MetOp-A minus NOAA-17 bias in Ch4 is $\sigma_\varepsilon / \sqrt{60}$ ~ 0.0015 K. The mean DD bias of -0.039 K thus appears statistically significant well beyond 99% confidence level ($\pm 3\sigma_\varepsilon$). These simple estimates demonstrate the accuracy potential of the DD technique to estimate cross-platform BT and SST biases.

Consistency between the conventional (Fig. 7, left) and robust (Fig. 7, right) DD statistics for NOAA-18 and MetOp-A indicates no gross errors in the ACSPO data for these platforms. The remaining small differences between the mean and median statistics can be used to further quantify the accuracy potential of the DD technique. Typically, these differences are within ~±0.01 K, in all cases. For instance, for MetOp-A Ch3B, the DD measures -0.008 K using the mean and +0.004 K using the median. Overall, the DD technique greatly reduces the effects of any BT and SST noises and is more effective to evaluate the cross-platform consistency than directly from Fig. 4 (cf. Strow et al., 2008). The largest inconsistency of 0.11 K is found in Ch4B between NOAA-18 and NOAA-17 using both mean and median statistics. Note also that the DD statistics in NOAA-16 is substantially improved when the median is used compared to the mean.

Another technique to check cross-platform consistency was developed at NESDIS for inter-calibrating the polar orbiting radiometers by using Simultaneous Nadir Overpasses (SNO, www.star.nesdis.noaa.gov/smcd/spb/calibration/sno/; c.f., Cao et al., 2004a; Tobin, 2008). Note that the tight space/time match-up is required by the SNO technique for polar-orbiting meteorological satellites, which limits the geographical domain in which it can be applied to two narrow high latitude ranges. In those areas, sensor is usually exposed to direct sun and therefore AVHRR calibration can be contaminated by the reflected solar radiation rendering this technique unusable for Ch3B and also limiting its potential for the longwave bands (Cao et al., 2001). Also, Ch3B data may not be available at the SNOs due to day/night switching of Ch3A/Ch3B. The SNO method would be more useful once the AVHRR radiances are recalibrated and these issues are resolved. The limitation of latitude was removed in the system set up at EUMETSAT for monitoring cross-platform consistency between IASI and geostationary Meteosat imagers (Hewison and König, 2008). However, the amount of match-up pixels still remains limited by the near-nadir conditions, time-window, and requirement of close proximity of the SEVIRI and IASI. The MICROS analyses, on the other hand, do include Ch3B with no limitation and allow validation of radiances in the full global domain including the mid-latitudes and Tropics. Also, using all-sky data may adversely affect the accuracy of SNO, when the pixel pairs being matched are in two satellite footprints, are not completely co-located. In MICROS, the cross-platform consistency is monitored in the whole global range by using the DD technique with CRTM as transfer standard, and the analyses are only concentrated in clear-sky domain. Thus, a much larger and more accurate and uniform statistics is obtained, which further reduces the noise and makes the statistics of the biases and DD signal near-Gaussian. Moreover, the DD technique in MICROS takes into account differences in spectral responses of different sensors, due to using

the CRTM as a transfer standard. Overall, the DD technique is promising to provide an effective and independent evaluation of sensor intercalibration, in addition to the SNO (Strow et al., 2008).

6. Conclusion and Future Work

The MICROS web-based tool was established to monitor global M-O biases in clear-sky brightness temperatures and SSTs over oceans in near-real time. In its functionality, it is similar to the other M-O monitoring systems in the operational use at the Numerical Weather Prediction Centers (e.g., Munro et al., 2004; Köpken et al., 2004; Garand et al., 2003) but is mostly SST-applications oriented. MICROS is an end-to-end system that processes satellite Level 1B data using ACSPO, performs statistical analyses of BTs and SSTs, and publishes their summaries on the web. Currently, AVHRR BTs in Ch3B, 4, and 5 from NOAA-16, -17, -18, and MetOp-A are monitored in MICROS. MICROS reports global maps, histograms, time series, and dependencies on the main factors using a conventional and robust statistics. Satellite-to-satellite double differences are also calculated and trended to facilitate cross-platform analyses. The DD technique used in MICROS can also contribute to validation of diurnal variability models and to establishing cross-sensor calibration links for the Global Space-Based Inter-Calibration System (GSICS, www.star.nesdis.noaa.gov/smcd/spb/calibration/icvs/GSICS/index.php). All analyses are performed separately for day and night, but only nighttime data were discussed in this paper.

From July to December 2008, the nighttime global BT biases have been fairly stable in all three AVHRR bands on NOAA-17, -18, and MetOp-A, even at the time of ACSPO version upgrades. Short-term variability in the BT and SST biases likely mostly arises from the instabilities in the Reynolds SST input. Generally, the BTs are cross-platform consistent to within several hundredths of a degree Kelvin, except for NOAA-18 Ch4, which is biased cold by ~-(0.09±0.02) K relative to NOAA-17 and MetOp-A. NOAA-16 is out-of-family and unstable. Analyses are underway to understand these anomalies.

Both conventional and robust statistics are implemented in MICROS. Robust statistics are more effective to evaluate the performance of sensor and CRTM, whereas the conventional statistics are useful to evaluate the overall product performance. Proximity of the two statistics is also a good indicator of the product quality.

Analyses of a six-month time series in MICROS revealed the need for improvement in three major areas. First, the daytime data are contaminated by the reflected signal, as is clearly evident from the MICROS web page. These data, therefore, were not analyzed in this study, pending major revision of the surface reflectance model adopted in CRTM. This work is currently underway jointly with the CRTM team and its results will be reported elsewhere. Second, satellite radiances should be reconciled, to minimize the need for an empirical bias correction in the physical SST retrieval and cloud screening algorithms. To that end, improvements to sensor radiances (including calibration and response functions) and accounting for the diurnal variability into cross-platform comparisons should improve the consistency in satellite radiances. Third, ACSPO processing should be improved (in particular, the SST and cloud mask algorithms). MICROS proved instrumental in identifying all these areas for improvements and to quantitatively measure the accuracy and consistency of ACSPO products, CRTM performance, and satellite radiances.

Work is also underway to extend MICROS functionality to include monitoring of BTs from MSG/SEVIRI. Data from NOAA-N' (NOAA-19), NPOESS/VIIRS, and GOES-R ABI will also be added to MICROS once they become available. Before physical SST retrievals in ACSPO are explored, daytime ACSPO analyses must be improved. In a longer perspective, we also plan to test the Goddard Chemistry Aerosol Radiation and Transport (GOCART) aerosols in conjunction with CRTM for improved SST. The effect of all new improvements and developments in ACSPO will be evaluated using the MICROS system.

Acknowledgements

This work is conducted under the Algorithm Working Group funded by the GOES-R Program Office, NPOESS Ocean Cal/Val project funded by IPO, and Polar PSDI and Ocean Remote Sensing programs funded by NESDIS. X. Liang also acknowledges the CIRA visiting scientist fellowship. CRTM is provided by the NESDIS Joint Center for Satellite Data Assimilation (JCSDA). Thanks to Yury Kihai for contribution in ACSPO granule collection, Feng Xu for help in web development, and Boris Petrenko for providing cloud mask. Thanks to Quanhua Liu, Yong Han, Yong Chen, Paul Van Delst, Fuzhong Weng, Changyong Cao, Likun Wang, and Nick Nalli of NOAA/NESDIS for advice and help. The views, opinions, and findings contained in this report are those of the authors and should not be construed as an official NOAA or U.S. Government position, policy, or decision.

References

Cao, C., M. Weinreb, and J. Sullivan (2001). Solar contamination effects on the infrared channels of the advanced very high resolution radiometer, *J. Geophys. Res*., 106, 33,463–33,469, doi:10.1029/2001JD001051.

Cao, C., M. Weinreb, and H. Xu (2004a). Predicting simultaneous nadir overpasses among polar-orbiting meteorological satellites for the intersatellite calibration of radiometers, *J. Atmos. Oceanic Technol.*, Vol. 21, pp. 537–542.

Cao, C., J. Sullivan, E. Maturi, and J. Sapper (2004b). The effect of orbit drift on the calibration of the 3.7 *m*m channel of the AVHRR onboard NOAA-14 and its impact on night-time sea surface temperature retrievals, *Int. J. Rem. Sens.,* Vol. 25, pp. 975-986.

Chen, Y. (2007). On the use of Planck-weighted transmittances in CRTM. CRTM document with CRTM version 1.1 release. www.star.nesdis.noaa.gov/sod/sst/micros/pdf/Planck-weight_transmittances_in_CRTM.pdf

Chou, M.D., W. L. Ridgway, and M. M.-H. Yan (1993). One-parameter scaling and exponential-sum fitting for water vapor and CO2 infrared transmission functions. *J. Atmos. Sci.,* 50, 2294–2303.

Dash, P., A. Ignatov, Y. Kihai, and J. Sapper (2009). The near-real time, web-based SST Quality Monitor (SQUAM): Application to NESDIS heritage AVHRR product. In preparation.

Gentemann, C. L. and P. J. Minnett (2008). Radiometric measurements of ocean surface thermal variability. *J. Geophys. Res.*, 113, C08017, DOI: 10.1029/2007JC004540.

Garand, L., (2003): Toward an integrated land-ocean surface skin temperature analysis from the variational assimilation of infrared radiances. *J. Appl. Meteor.,* 42, 570–583.

Han, Y., P. van Delst, Q. Liu, F. Weng, B. Yan, R. Treadon, and J. Derber (2006). JCSDA Community Radiative Transfer Model (CRTM) – Version 1. *NOAA Technical Report NESDIS 122*. www.orbit2.nesdis.noaa.gov/sod/sst/micros/pdf/CRTM_v1_NOAAtechReport-1.pdf

Hewison, T.J., and M. König, (2008). Inter-Calibration of Meteosat Imagers and IASI, *Proceedings of EUMETSAT Satellite Conference*, Darmstadt, Germany. tim.zymurgy.org/hewison/pdf_gsics_pres_04_proceedings.pdf

Ignatov, A., J. Sapper, I. Laszlo, N. Nalli, A. Harris, W. Pichel, A.E. Strong, E. Bayler, X. Li, and E. Maturi (2004). Global operational sea surface temperature and aerosol products from AVHRR: Current status, diagnostics, and potential enhancements, paper presented at 13th AMS Conference on Satellite Oceanography and Meteorology, Am. Meteorol. Soc., Norfolk, VA.

Kleespies, T.J., P. van Delst, L.M. McMillin, and J. Derber (2004). Atmospheric transmittance of an absorbing gas. 6. An OPTRAN Status Report and Introduction to the NESDIS/NCEP Community Radiative Transfer Model. *Appl. Opt.*, 43, 3103–3109.

Köpken, C., G. Kelly, and J.-N. Théapaut (2004). Assimilation of Meteosat radiance data within the 4D-Var system at ECMWF: assimilation experiments and forecast impact. *Q. J. R. Meteorol. Soc.*, 130, 2277–2292.

Kennedy, J. J., P. Brohan, and S.F.B. Tett (2007). A global climatology of the diurnal variations in sea-surface temperature and implications for MSU temperature trends. *Geophy. Res. Let*, 34, L05712, doi:10.1029/2006GL028920.

Liang, X., A. Ignatov, and Y. Kihai (2009). Implementation of the Community Radiative Transfer Model (CRTM) in Advanced Clear-Sky Processor for Oceans (ACSPO) and validation against nighttime AVHRR radiances. *J. Geophys. Res.*. 114, D06112, doi:10.1029/2008JD010960.

Liu, Q. (2008). Personal communication.

Liu, Q, X. Liang, Y. Han, P. van Delst, Y. Chen, A. Ignatov, and F. Weng (2009). Effect of out-of-band response in NOAA-16 AVHRR Channel 3B on top-of-atmosphere radiances calculated with the Community Radiative Transfer Model. Accepted for publication in *J. Atmos. Oceanic Technol.* March 2009.

May, D.A., M.M. Parmeter, D.S. Olszewski, and B.D. McKenzie (1998). Operational processing of satellite sea surface temperature retrievals at the Naval Oceanographic Office. *Bulletin of the American Meteorological Society*, 79, 397–407.

Merchant, C.J., P. Le Borgne, H. Roquet, and A. Marsouin (2009). Sea surface temperature from a geostationary satellite by optimal estimation. *Remote Sens. Environ*., 113, 445–457.

Merchant, C. J., P. Le Borgne, A. Marsouin, and H. Roquet (2008). Optimal estimation of sea surface temperature from split-window observations. *Remote Sens. Environ*., 112, 2469–2486.

Munro, R., C. Köpken, G. Kelly, J.-N. Théapaut, and R. Saunders (2004). Assimilation of Meteosat radiance data within the 4D-Var system at ECMWF: data quality monitoring, bias correction, and single-cycle experiments. *Q. J. R. Meteorol. Soc.,* 130, 2293–2313.

Petrenko, B., A. Heidinger, A. Ignatov, and Y. Kihai (2008). Clear-sky mask for the AVHRR Clear-Sky Processor for Oceans. Ocean Sciences Meeting, 2–7 March 2008, Orlando, FL. www.star.nesdis.noaa.gov/sod/osb/sst/ignatov/conf/index.html

Petrenko, B., A. Ignatov, Y. Kihai, X. Liang, N. Shabanov, and A. Heidinger (2009). Cloud mask and quality control for SST within the Advanced Clear Sky Processor for Oceans (ACSPO), 38th AMS Annual meeting, Phoenix, AZ.

Reynolds, R.W., N.A. Rayner, T.M. Smith, D.C. Stokes, and W. Wang (2002). An improved *in situ* and satellite SST analysis for climate. *J. Clim.*, 15, 1609–1625.

Reynolds, R.W., T.M. Smith, C. Liu, D.B. Chelton, K.S. Casey, and M.G. Schlax (2007). Daily high-resolution blended analyses for sea surface temperature. *J. Clim.*, 20, 5473–5496.

Strow, L.L., S. Hannon, and D. Tobin (2008). AIRS and IASI validation and intercomparisons with SARTA, Advanced High Spectral Resolution Infrared Observations Workshop, EUMETSAT, Darmstadt, Germany, 15–17 September 2008. www.ssec.wisc.edu/hsr/meetings/2008/presentations/Larrabee_Strow.pdf

Stuart-Menteth, A.C., I.S. Robinson, and R.A. Weller (2005). Sensitivity of the diurnal warm layer to meteorological fluctuations part 2: A new parameterisation for diurnal warming. *J. Atmos. Ocean Sci*., 10, 209–234.

Tobin, D., (2008). An SNO analysis of IASI and AIRS spectral radiance, *GSICS Quarterly*, Vol. 2, No. 3.

Turner, D.S. (2000). Systematic errors that are due to the monochromatic-equivalent radiative transfer approximation in thermal emission problems. *Appl. Opt.,* 39,5663–5670.

Wang, L., X. Wu, Y. Li, M. Goldberg, S-H. Sohn, and C. Cao (2009). Comparison of AIRS and IASI radiances using GOES imagers as transfer radiometers towards climate data records. Submitted to *J. Appl. Meteor. Clim.*

Watts, P. D., M. R. Allen, and T. J. Nightingale (1996). Wind speed effects on sea surface emission and reflection for the Along Track Scanning Radiometer. *J. Atmos. Oceanic Technol.*, 13, 126–141.

Wu, A., X. Xiong, and C. Cao (2008). Terra and Aqua MODIS inter-comparison of three reflective solar bands using AVHRR onboard the NOAA-KLM satellites. *Int. J. Rem. Sens.,* 29, 1997–2010.

Wu, X. and W. L. Smith (1997). Emissivity of rough sea surface for 8–13 um: modeling and verification. *Appl. Opt.*, 36, 2609–2618.

Figures

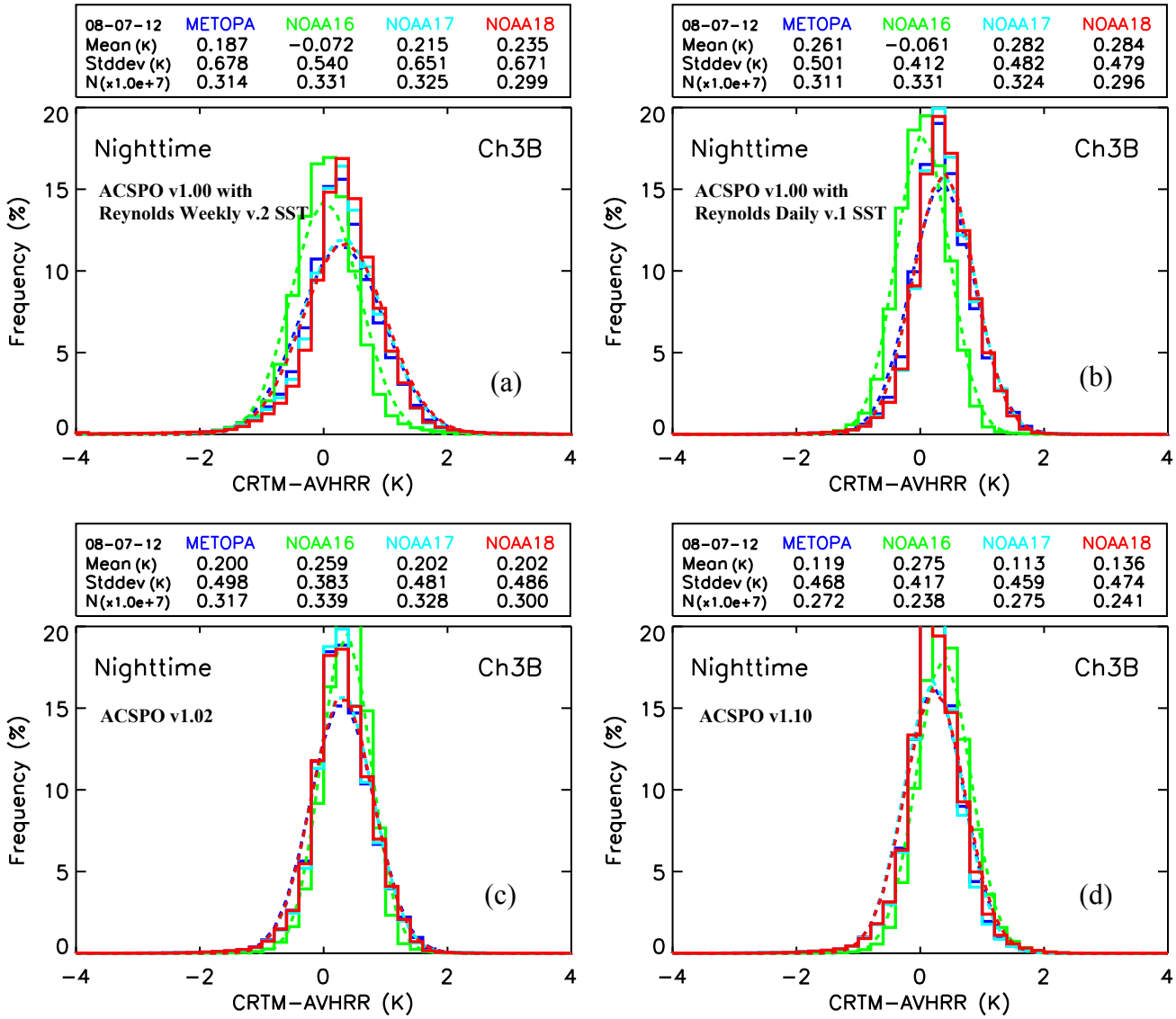

Figure 1. Global histograms of the M-O BT biases for 24 hours of nighttime data on 12 July 2008 in AVHRR Ch3B onboard MetOp-A and NOAA16-18. (a-b) ACSPO v1.00 with (a) Reynolds weekly 1° v2.0 SST and (b) Reynolds daily 0.25° v1.0 SST (AVHRR-based) as CRTM input (CRTM r577 was used in both cases); (c) ACSPO v1.02 (same as (b) but using CRTM v1.1); (d) ACSPO v1.10 (same as (c) but using upgraded cloud mask).

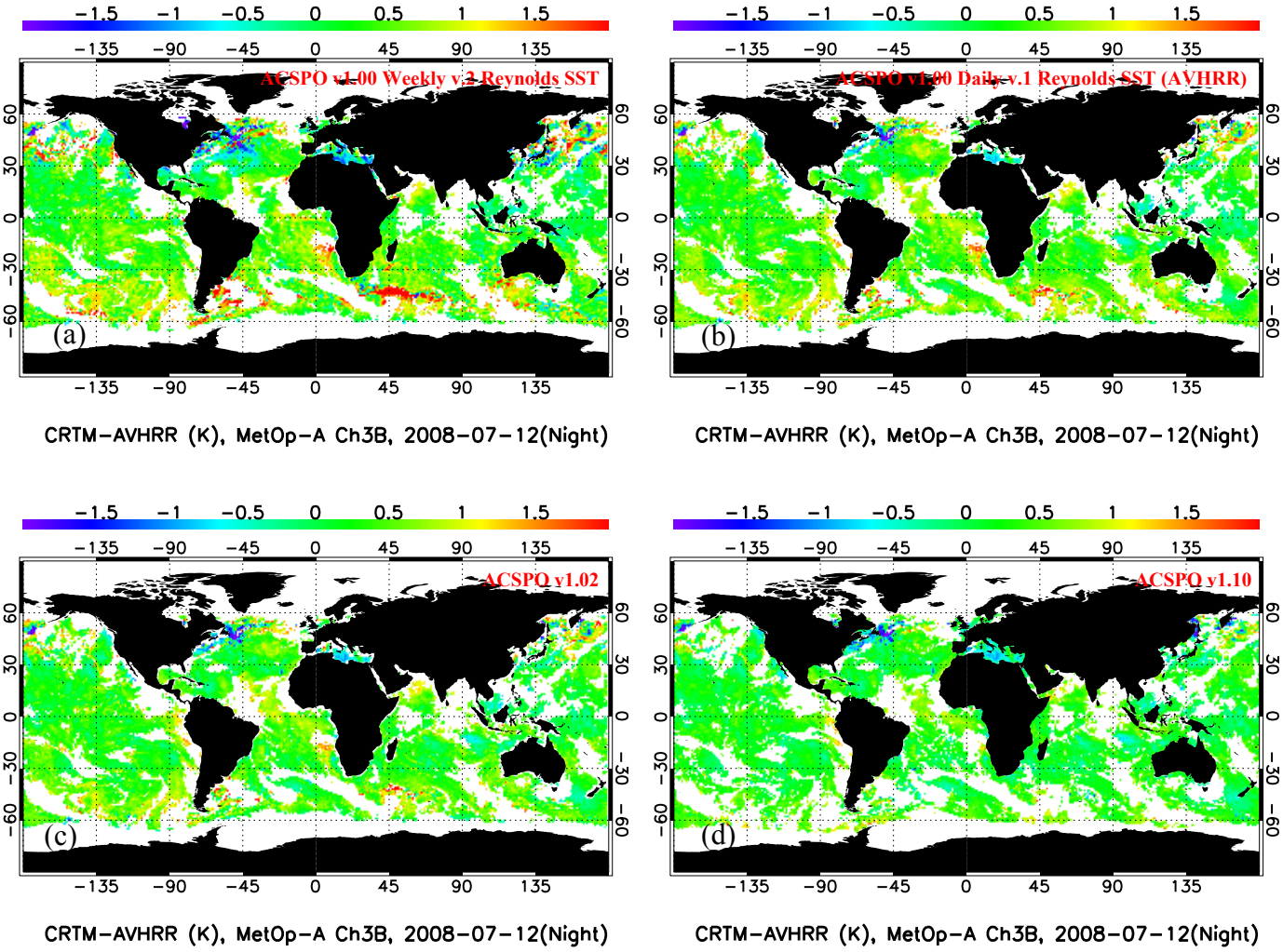

Figure 2. Global geographic distributions of the M-O BT biases in MetOp-A Ch3B. Otherwise as in Fig. 1.

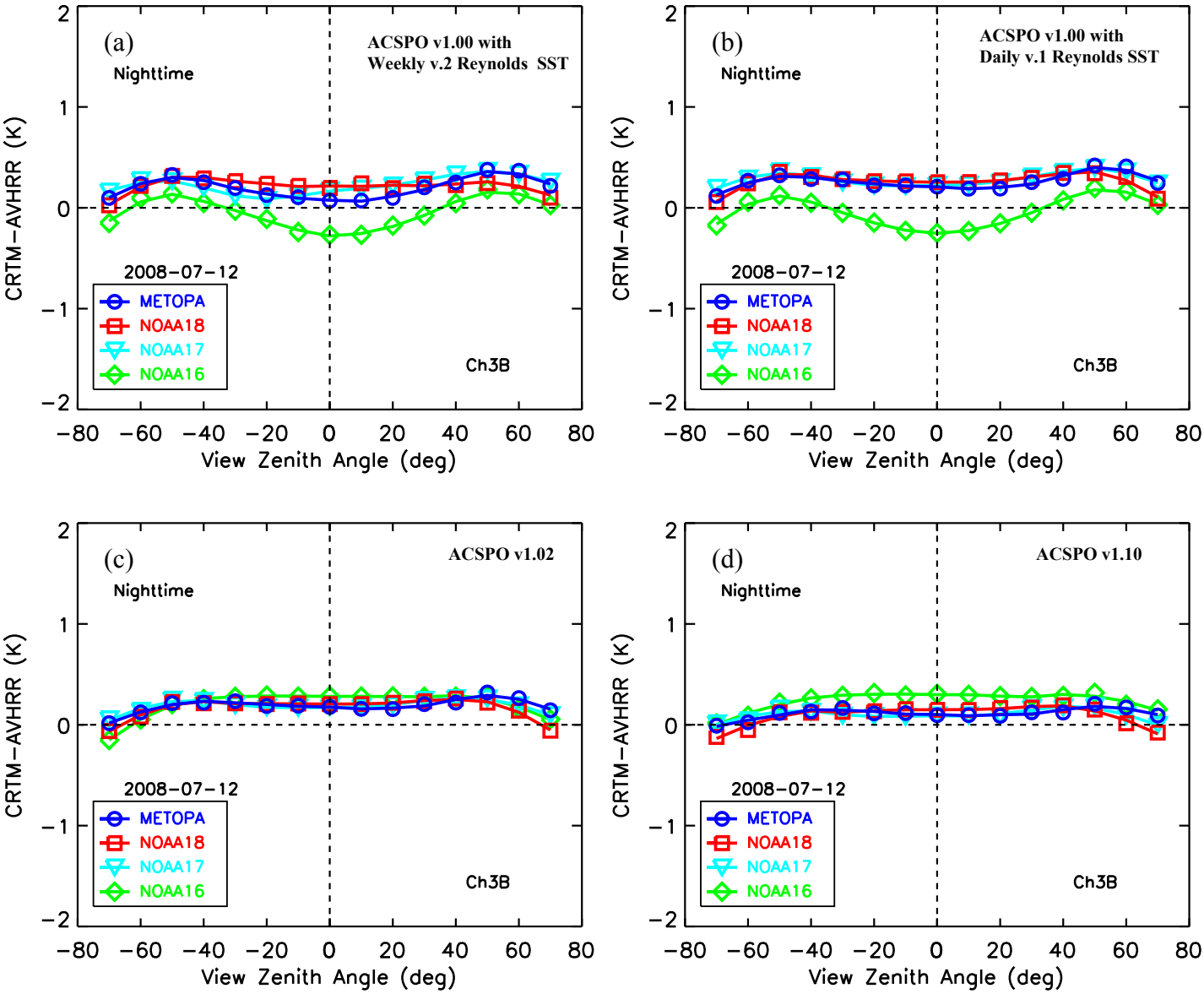

Figure 3. View zenith angle dependencies of the M-O BT biases. Otherwise as in Fig. 1.

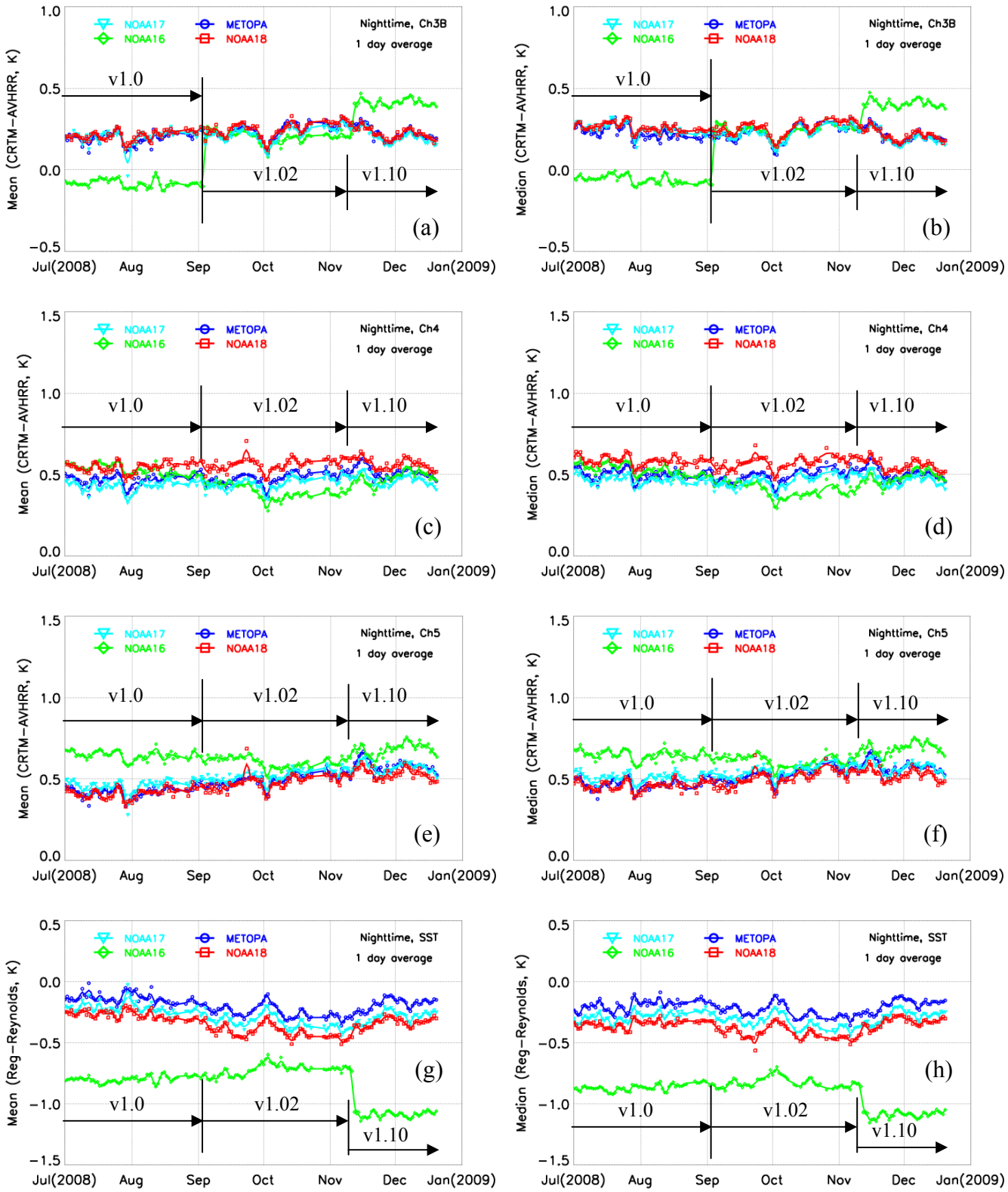

Figure 4. Time series of the global M-O (left) mean and (right) median BT biases in AVHRR (a-b) Ch3b, (c-d) Ch4, (e-f) Ch5, and (g-h) SSTs. Each point in the graphs represents the statistics derived from all nighttime data within a 24-hour interval. ACSPO versions are overlaid.

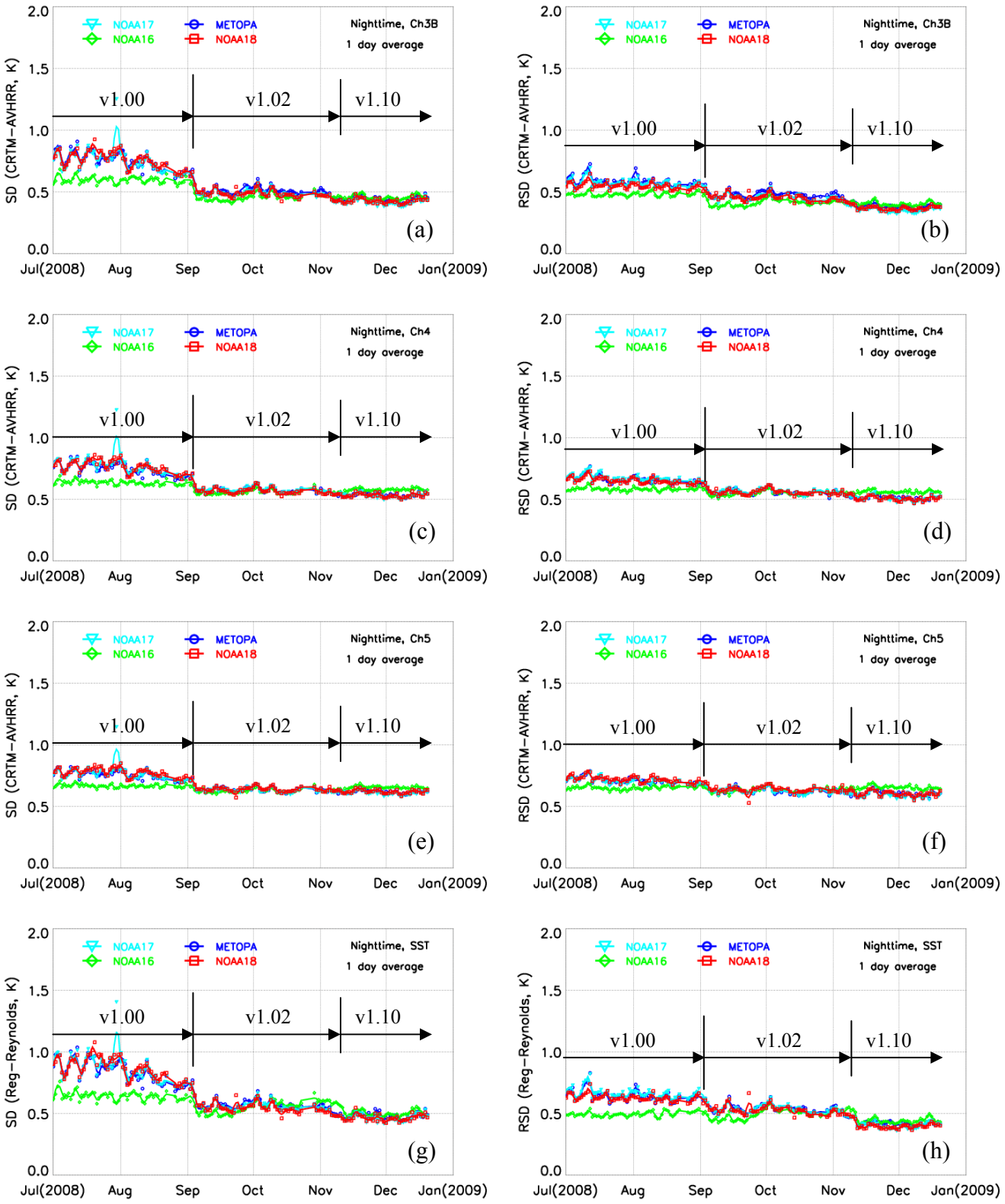

Figure 5. Time series of (left) conventional (SD) and (right) robust standard deviations (RSD). Otherwise as in Fig. 4.

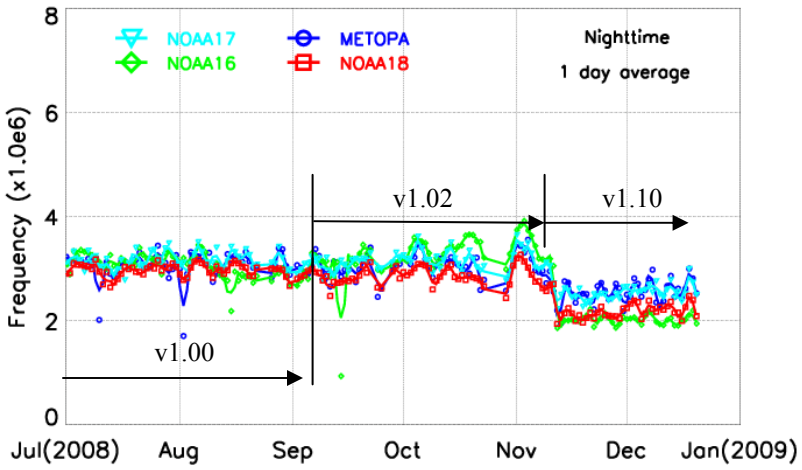

Figure 6. Time series of the ACSPO sample size. Otherwise as in Fig. 4.

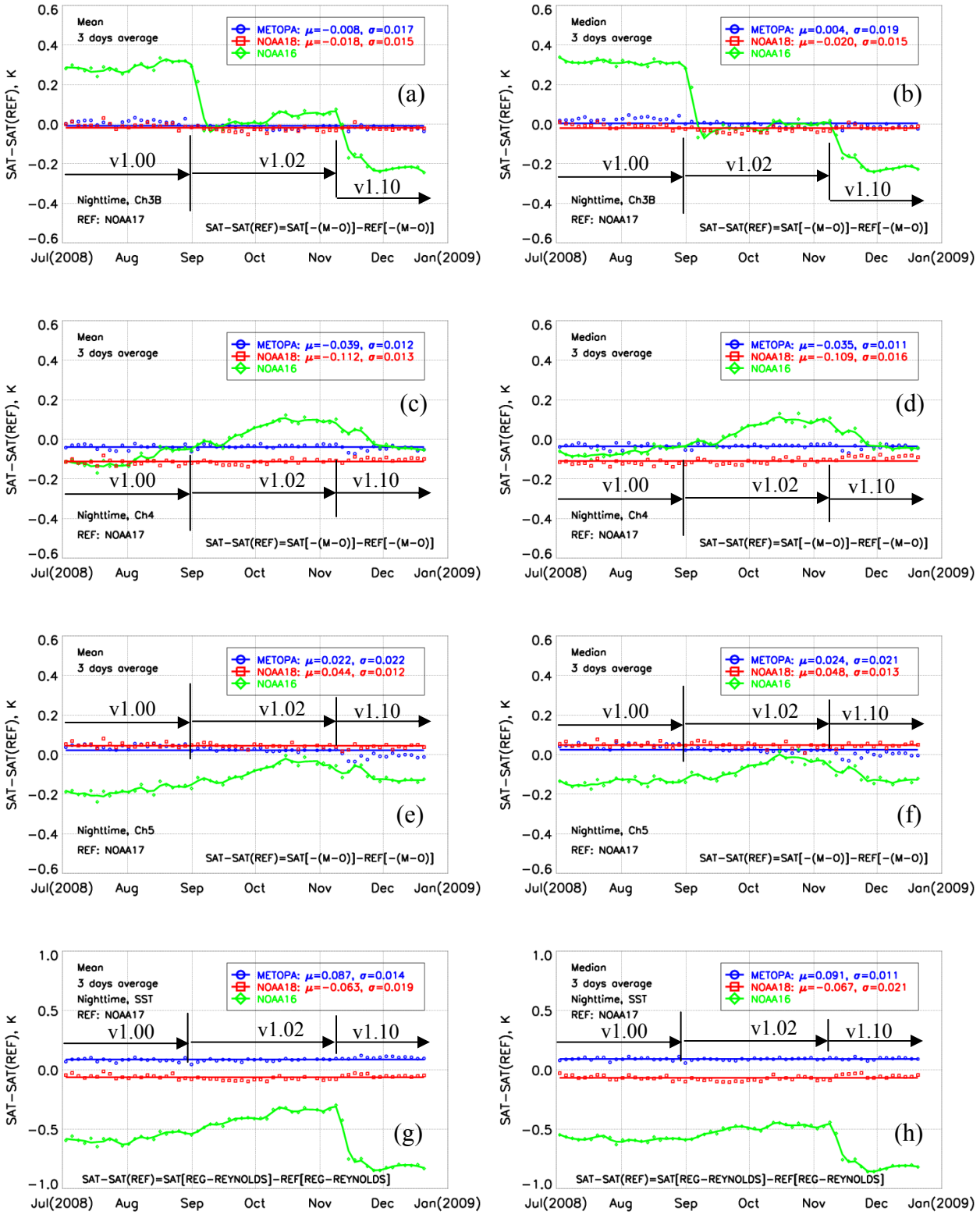

Figure 7. Cross-platform double-differences in AVHRR (a-b) Ch3b, (c-d) Ch4, (e-f) Ch5, and (g-h) SSTs, using (left) mean and (right) median statistics. Data are smoothed out by a three-day moving averaging filter to suppress noise and rectify signal. Mean values of the cross-platform biases and their corresponding day-to-day standard deviations are also shown. Otherwise as in Fig. 4.